

The upper Miocene Deurne Member of the Diest Formation revisited: unexpected results from the study of a large temporary outcrop near Antwerp International Airport, Belgium

Supplementary material 2: Additional details on the lab analyses and techniques used

STIJN GOOLAERTS^{1,*}, JEF DE CEUSTER², FREDERIK H. MOLLEN³, BERT GIJSEN³, MARK BOSSELAERS¹, OLIVIER LAMBERT¹, ALFRED UCHMAN⁴, MICHAEL VAN HERCK⁵, RIEKO ADRIAENS⁶, RIK HOUTHUYSEN⁷, STEPHEN LOUWYE⁸, YAANA BRUNEEL⁵, JAN ELSSEN⁵ & KRISTIAAN HOEDEMAKERS¹

¹ OD Earth & History of Life, Scientific Heritage Service and OD Natural Environment, Royal Belgian Institute of Natural Sciences, Belgium; stijn.goolaerts@naturalsciences.be; mark.bosselaers@telenet.be; olambert@naturalsciences.be; kristiaan.hoedemakers@naturalsciences.be.

² Veldstraat 42, 2160 Wommelgem, Belgium; jeffdeco@gmail.com.

³ Elasmobranch Research Belgium, Rehaegenstraat 4, 2820 Bonheiden, Belgium; frederik.mollen@gmail.com; bert.gijsen@skynet.be.

⁴ Faculty of Geography and Geology, Institute of Geological Sciences, Jagiellonian University, Gronostajowa 3a, 30-387 Kraków, Poland; alfred.uchman@uj.edu.pl.

⁵ Department of Earth & Environmental Sciences, KU Leuven, Belgium; michiel.vanherck@student.kuleuven.be; yaana.bruneel@kuleuven.be; jan.elsen@kuleuven.be.

⁶ Q Mineral, Heverlee, Belgium; radriaens@qmineral.com.

⁷ Independent consultant, Halle, Belgium; rik.houthuys@telenet.be.

⁸ Department of Geology, Campus Sterre, S8, Krijgslaan 281, 9000 Gent, Belgium; stephen.louwye@ugent.be.

* corresponding author.

ABSTRACT. A 5.50 m thick interval of fossiliferous intensely bioturbated heterogenous glauconiferous sand of the upper Miocene Diest Formation is documented from a very large temporary outcrop just southeast of Antwerp International Airport (northern Belgium), allowing to observe lateral variations over several hundreds of meters and to collect many vertebrate and invertebrate fossils. This paper documents observations on lithology, sedimentary and post-sedimentary structures, and discusses the results of the multi-proxy analyses of the sediment (grain size, glauconite content, clay mineralogy, Fe content and $\text{Fe}^{3+}/\text{Fe}^{2+}$ ratios), the interpretation of the trace fossil assemblage and the sedimentary structures as well as of the large-scale samplings of micro-, meso- and macrofossils. We evidence that the Diest Formation in the Antwerp area consists of two different lithological entities, and that this twofold character can be extrapolated to all previously recorded Deurne Member outcrops. A revised lithostratigraphic scheme for the Diest Formation in the Antwerp area is proposed, with the new Borsbeek member at the base and a redefined Deurne Member at the top.

For full text, see: <https://doi.org/10.20341/gb.2020.011>

1. Coding of (sub)samples

All samples analyzed at the laboratory of the KU Leuven Department of Earth & Environmental Sciences (EES) are subsamples of the master sample set deposited at the Royal Belgian Institute of Natural Sciences (RBINS) under I.G. 33969. Upon their arrival, these subsamples received an additional coding of the sample database of the Geology research group of the Dept. EES, and yet another additional coding for those samples analyzed in the chemistry lab of the Dept. EES. The correlation matrix between the sample numbers is given below.

Table 1. Coding of subsamples and their position in the section.

Sample N°	Subsample N° database EES KU Leuven	Subsample N° chemistry lab EES KU LEUVEN	Depth in section (m)	Depth towards TAW (m)	Formation	Member
LP1-01	DE18VH01	M-2	0.3	3.7	Berchem	Antwerpen
LP1-02	DE18VH02	M-3	0.4	3.8	Berchem	Antwerpen
LP1-03	DE18VH03	M-4	0.6	4.0	Berchem	Antwerpen
LP1-04	DE18VH04	M-5	0.9	4.3	Berchem	Antwerpen
LP1-06	DE18VH05	M-6	1.3	4.7	Berchem	Antwerpen
LP1-07	DE18VH06	M-7	1.5	4.9	Diest	Unit 1
LP1-08	DE18VH07	M-1	1.6	5.0	Diest	Unit 1
LP1-09	DE18VH08	M-8	1.7	5.1	Diest	Unit 1
LP1-10	DE18VH09	M-9	1.9	5.3	Diest	Unit 1
LP1-11	DE19VH01	M-12	2.5	5.9	Diest	Unit 1
LP1-12	DE18VH10	M-10	3.0	6.4	Diest	Unit 1
LP1-13	DE18VH11	M-11	3.5	6.9	Diest	Unit 1
LP1-14	DE19VH02	M-13	3.7	7.1	Diest	Unit 1
LP1-15	DE19VH03	M-14	4.2	7.6	Diest	Unit 1
LP1-16	DE19VH04	M-15	4.5	7.9	Diest	Unit 1
LP1-17	DE19VH05	M-16	5.0	8.4	Diest	Unit 2
LP1-18	DE19VH06	M-17	5.2	8.6	Diest	Unit 2
LP1-19	DE19VH07	M-18	5.5	8.9	Diest	Unit 2
LP1-20	DE19VH08	M-19	6.1	9.5	Diest	Unit 2
LP1-26	DE19VH09	M-20	1.5	4.9	Berchem	Antwerpen
LP2-15	DE19VH10	M-21	4.0	7.4	Diest	Unit 1
LP2-16	DE19VH11	M-22	4.2	7.6	Diest	Unit 1
LP2-17	DE19VH12	M-23	4.4	7.8	Diest	Unit 1
LP2-18	DE19VH13	M-24	4.7	8.1	Diest	Unit 1
LP2-19	DE19VH14	M-25	5.2	8.6	Diest	Unit 1
LP1-50	DE19VH15	M-26	2.7	6.1	Diest	Unit 2
LP1-61	DE19VH16	M-27	3.8	7.2	Diest	Unit 1
LP1-62	DE19VH17	/	4.2	7.6	Diest	Unit 1
LP1-63	DE19VH18	/	4.8	8.2	Diest	Unit 1
LP1-64	DE19VH19	/	5.0	8.4	Diest	Unit 1

2. Fe-content: techniques used, calibration and results

The phenanthroline method was used for determination of the Fe²⁺ and total Fe content. The colorimetric determination of Fe²⁺ through 1,10-phenanthroline (Shapiro, 1960; Fritz & Popp, 1985) allows determination of both Fe²⁺ and total Fe contents in a single dissolved rock sample. The samples are dissolved by a solution of HF and H₂SO₄ in the presence of 1,10-phenanthroline. This organic reagent forms an orange-colored complex with Fe²⁺, which both prevents the oxidation of Fe²⁺ to Fe³⁺ and allows for a colorimetric determination of Fe²⁺ (at 555 nm with UV-VIS). The intensity of the complex is directly proportional to the Fe²⁺ content of the digested rock sample (Fritz and Popp, 1985). After the UV-VIS measurement the solutions are analyzed by atomic absorption spectroscopy (AAS) to determine the total Fe content (at 248 nm). Both analyses make use of a calibration curve using geological Standard Reference Materials (SRMs) to determine the mass percentages Fe²⁺ and total Fe. For a good quantification it is necessary to select SRM's in the range of the expected Fe²⁺ and Fe tot content of the samples. For this dataset the SRM's NIM-S, NIM-G, GSP-1, SY-3, DR-N, MRG-1 and BCR-1 were selected.

The samples need to be milled and homogenous as only 10 mg is needed for the analysis. The samples were dry milled in a ball mill using tungstencarbide milling elements. A possible complication of the method arises when no Fe²⁺ is present, in that case phenanthroline forms a complex with part of the Fe³⁺.

Table 2. Results of UV-VIS and AAS. Mean iron content calculated per lithostratigraphic unit. Standard deviation has been abbreviated to S.D.

	Fe ²⁺	S.D.	Fe ³⁺	S.D.	Fe tot	S.D.
Formation	mg/g	mg/g	mg/g	mg/g	mg/g	mg/g
Diest LP1	8.86	1.65	71.0	8.97	79.8	10.00
Diest LP2	8.08	1.38	63.3	7.03	71.4	7.52
Berchem LP1	9.13	1.57	74.3	8.10	83.4	9.34
Member						
Antwerpen LP1	9.13	1.57	74.3	8.10	83.4	9.34
Unit 1 LP1	9.49	1.38	73.2	9.23	82.7	9.92
Unit 1 LP2	8.10	1.39	62.7	7.29	70.8	7.72
Unit 2 LP1	7.12	0.88	64.7	3.71	71.8	4.32
Unit 2 LP2	8.45		62.7		71.1	

Table 3. Results of SRM's including accuracy

	Mean absorption	Concentration measured	Concentration theoretical	Accuracy
		mg/L	mg/L	%
NIM-S	0.110	3.012	2.84	94.293
NIM-G	0.144	4.087	3.68	90.044
GSP-1	0.261	7.955	7.86	98.808
SY-3	0.444	14.558	13.41	92.114

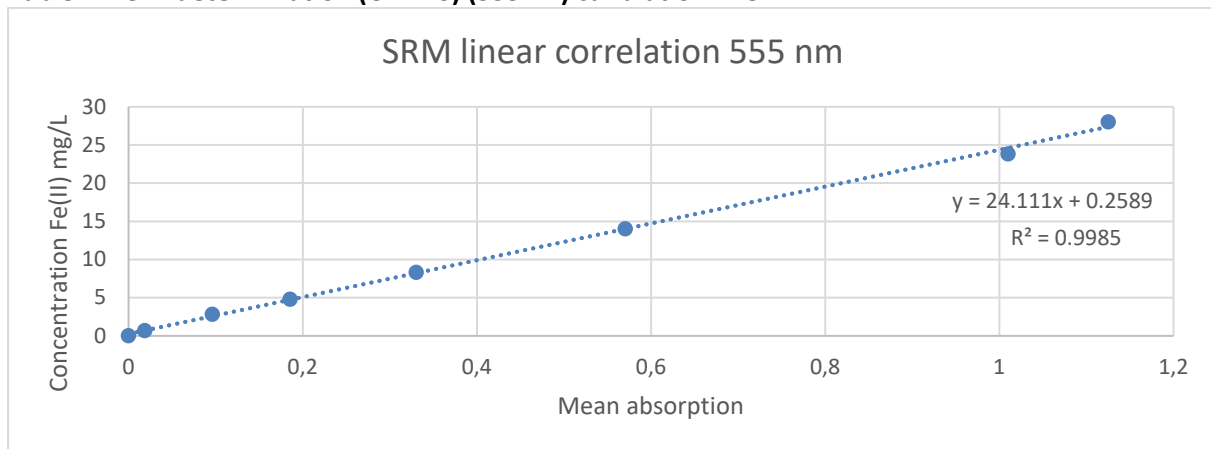
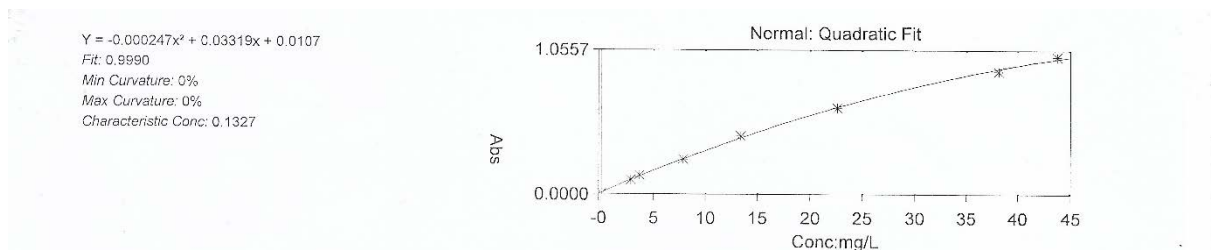
Table 4. Precision of the AAS measurements Table 5. Precision of the UV-VIS measurements

Precision AAS		
Labo code	Concentration	Precision
	mg/L	%
M-12A	21.788	
M-12B	22.904	4.873
M-20A	26.960	
M-20B	27.697	2.659
M-30A	18.626	
M-30B	18.202	2.330

Precision UV-VIS		
Labo code	Concentration	Precision
	mg/L	%
M-12A	2.718	
M-12B	2.823	3.701
M-20A	3.369	
M-20B	3.206	4.830
M-30A	2.357	
M-30B	2.292	2.805

Table 6. Flame AAS set up details

ANALYSIS INFORMATION	NAME	OPERATOR	TIME	DATE	Spectrometer:	
	Analysis 1	AAS	14:13:21	19/03/2019	S Series 711443 v1.23	
GENERAL PARAMETERS	Instrument Mode:	Flame	Autosampler :	None		
	Dilution:	None	Use SFI:	No		
SPECTROMETER PARAMETERS	Element:	Fe	Measurement Mode:	Absorbance		
	Wavelength:	248.3	Bandpass:	0.2nm	Lamp Current: %	75
	Background Correction:	D2	High Resolution:	Off	Optimise Spectrometer Parameters:	No
	Signal Type:	Continuous	Resamples:	Fast	Number Of Resamples:	3
	Measurement Time: secs		3 Flier Mode:	No		
	Use RSD Test:	No				
FLAME PARAMETERS	Flame Type:	Air-C2H2	Fuel Flow: L/min	0.9	Auxiliary Oxidant:	Off
	Nebuliser Uptake: secs		4 Burner Stabilisation: mins	0	Optimise Fuel Flow:	No
	Burner Height: mm		7 Optimise Burner Height:	No		

Table 7. Fe²⁺ determination (UV-VIS) (555nm) calibration line**Table 8. Fe total determination (Flame AAS) (248nm) calibration line****Table 9. Standards used in UV-VIS mass and concentration**

Chemistry Lab Code	Weight mg	Fe ²⁺ (UV-VIS) mg/L	Fe total (AAS) mg/L
NIM-S	14.8	0.69	2.90
NIM-G	14.0	2.83	3.96
GSP-1	13.2	4.80	7.92
SY-3	14.9	8.32	13.53
DR-N	16.7	14.02	22.66
MRG-1	17.7	23.83	44.14
BCR-1	20.3	28.02	38.08

Table 10. Limit of detection of Flame-AAS measurements

AAS limit of detection	
Sample Code	Concentration mg/L
Blank	-0.3475
Blank	-0.3448
Blank	-0.3340
Blank	-0.3278
Blank	-0.3510
Blank	-0.3165
Blank	-0.3434
Blank	-0.3157
Limit of detection	-0.2962

Table 11. Results

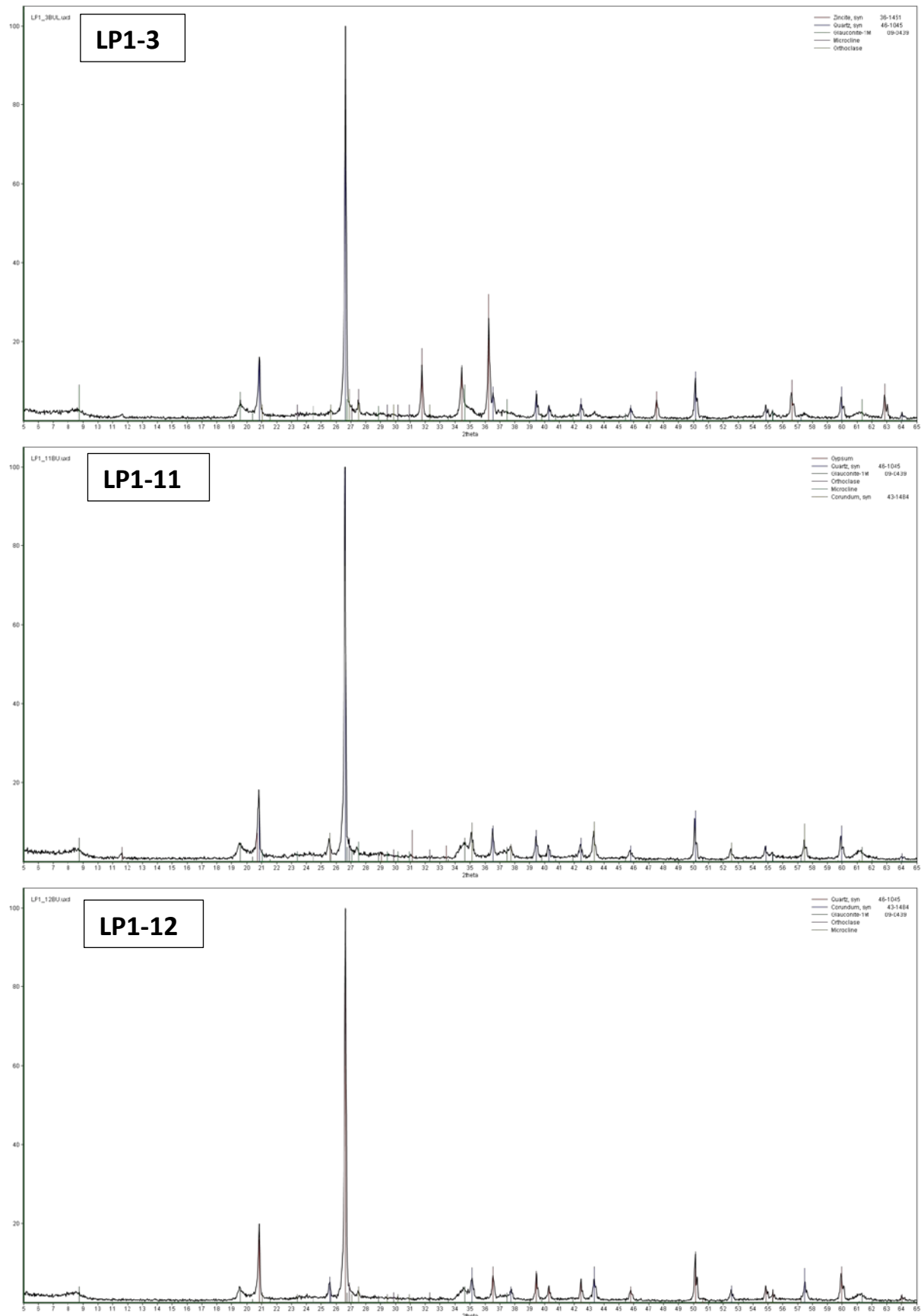
Chemistry Lab Code	Sample N°	Sample N° KU Leuven database	Depth section	Formation	Member	Weight sample	Fe2+	Fe2+	Fe tot	Fe tot	Fe3+	Fe2+/ Fe tot	Fe3+/ Fe tot	Fe2+/ Fe3+
			m			mg	mg/L	mg/g	mg/L	mg/g	mg/g	%	%	%
M-2	LP1-01	DE18VH01	0.3	Berchem	Antwerpen	13.8	2.332	8.451	21.952	79.538	71.087	0.106	0.894	0.119
M-3	LP1-02	DE18VH02	0.4	Berchem	Antwerpen	14.8	2.670	9.020	27.162	91.763	82.743	0.098	0.902	0.109
M-4	LP1-03	DE18VH03	0.6	Berchem	Antwerpen	13.0	1.826	7.024	20.231	77.812	70.789	0.090	0.910	0.099
M-5	LP1-04	DE18VH04	0.9	Berchem	Antwerpen	13.0	2.067	7.951	18.121	69.695	61.744	0.114	0.886	0.129
M-6	LP1-06	DE18VH05	1.3	Berchem	Antwerpen	14.7	2.549	8.672	22.349	76.016	67.345	0.114	0.886	0.129
M-7	LP1-07	DE18VH06	1.5	Diest	Unit 1	13.7	2.586	9.437	26.952	98.363	88.927	0.096	0.904	0.106
M-20A	LP1-26	DE19VH09	1.5	Berchem	Antwerpen	14.1	3.369	11.948	26.960	95.604	83.657	0.125	0.875	0.143
M-20B	LP1-26	DE19VH09	1.5	Berchem	Antwerpen	14.8	3.206	10.833	27.697	93.571	82.738	0.116	0.884	0.131
M-1	LP1-08	DE18VH07	1.6	Diest	Unit 1	13.3	3.152	11.850	24.016	90.286	78.435	0.131	0.869	0.151
M-8	LP1-09	DE18VH08	1.7	Diest	Unit 1	13.2	2.284	8.652	20.177	76.427	67.775	0.113	0.887	0.128
M-9	LP1-10	DE18VH09	1.9	Diest	Unit 1	13.0	2.718	10.455	26.453	101.743	91.288	0.103	0.897	0.115
M-12A	LP1-11	DE19VH01	2.5	Diest	Unit 1	13.2	2.718	10.296	21.788	82.529	72.233	0.125	0.875	0.143
M-12B	LP1-11	DE19VH01	2.5	Diest	Unit 1	13.8	2.823	10.227	22.904	82.984	72.757	0.123	0.877	0.141
M-26	LP1-50	DE19VH15	2.7	Diest	Unit 2	13.3	2.248	8.451	18.915	71.109	62.657	0.119	0.881	0.135
M-10	LP1-12	DE18VH10	3.0	Diest	Unit 1	14.5	2.429	8.375	24.110	83.136	74.761	0.101	0.899	0.112
M-11	LP1-13	DE18VH11	3.5	Diest	Unit 1	14.5	3.122	10.766	22.155	76.398	65.632	0.141	0.859	0.164
M-13	LP1-14	DE19VH02	3.7	Diest	Unit 1	13.1	2.509	9.577	20.311	77.523	67.946	0.124	0.876	0.141
M-27	LP1-61	DE19VH16	3.8	Diest	Unit 1	14.7	2.831	9.628	26.877	91.418	81.790	0.105	0.895	0.118

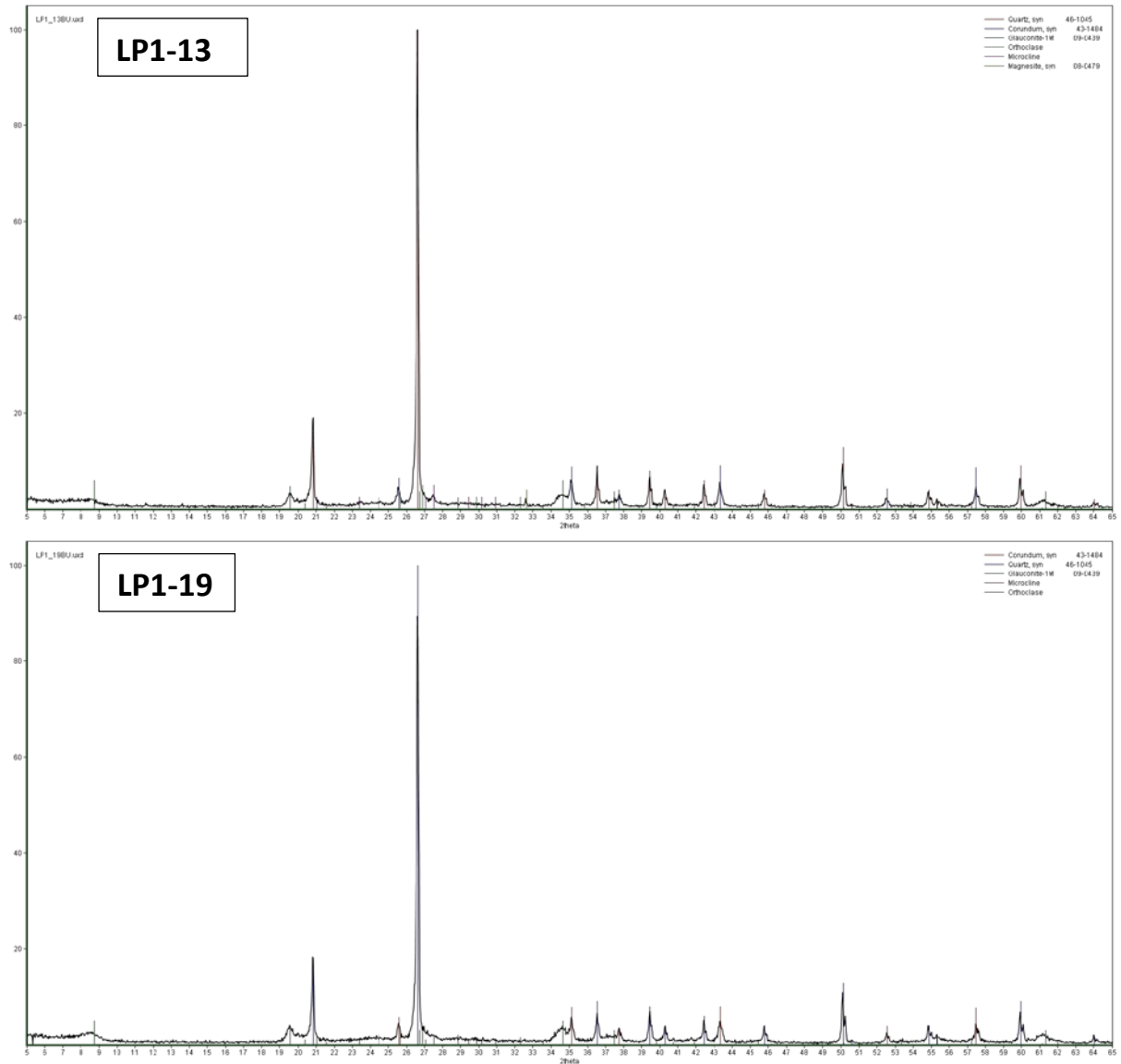
Chemistry Lab Code	Sample N°	Sample N° database KU Leuven	Depth in section	Formation	Member	Sample Weight	Fe2+	Fe2+	Fe tot	Fe tot	Fe3+	Fe2+/ Fe tot	Fe3+/ Fe tot	Fe2+/ Fe3+
			m			Mg	mg/L	mg/g	mg/L	mg/g	mg/g	%	%	%
M-21	LP2-15	DE19VH10	4.0	Diest	Unit 1	14.4	1.778	6.173	19.727	68.495	62.322	0.090	0.910	0.099
M-14	LP1-15	DE19VH03	4.2	Diest	Unit 1	13.2	1.778	6.734	18.855	71.420	64.685	0.094	0.906	0.104
M-22	LP2-16	DE19VH11	4.2	Diest	Unit 1	13.8	1.874	6.791	18.866	68.354	61.563	0.099	0.901	0.110
M-28	LP1-62	DE19VH17	4.2	Diest	Unit 1	13.3	1.995	7.500	20.474	76.971	69.472	0.097	0.903	0.108
M-23	LP2-17	DE19VH12	4.4	Diest	Unit 1	13.3	2.320	8.723	17.462	65.645	56.921	0.133	0.867	0.153
M-15	LP1-16	DE19VH04	4.5	Diest	Unit 1	14.8	2.369	8.002	20.480	69.189	61.187	0.116	0.884	0.131
M-24	LP2-18	DE19VH13	4.7	Diest	Unit 1	13.8	2.308	8.364	19.494	70.632	62.268	0.118	0.882	0.134
M-16	LP1-17	DE19VH05	5.0	Diest	Unit 2	12.8	1.826	6.430	18.360	64.646	58.216	0.099	0.901	0.110
M-30A	LP1-64	DE19VH19	5.0	Diest	Unit 1	14.4	1.718	6.709	17.664	68.999	62.290	0.097	0.903	0.108
M-30B	LP1-64	DE19VH19	5.0	Diest	Unit 1	13.7	2.357	8.182	18.626	64.674	56.491	0.127	0.873	0.145
M-17	LP1-18	DE19VH06	5.2	Diest	Unit 2	13.7	2.292	8.366	18.202	66.431	58.065	0.126	0.874	0.144
M-25	LP2-19	DE19VH14	5.2	Diest	Unit 1	13.7	1.874	6.841	18.347	66.959	60.118	0.102	0.898	0.114
M-18	LP1-19	DE19VH07	5.5	Diest	Unit 2	13.4	2.983	10.888	19.507	71.192	60.303	0.153	0.847	0.181
M-19	LP1-20	DE19VH08	6.1	Diest	Unit 2	13.8	2.308	8.613	20.986	78.306	69.693	0.110	0.890	0.124

3. Mineralogical analyses: techniques used, calibration and results

Philips PW1830 diffractometer with Bragg/Brentano θ - 2θ setup, CuK α radiation, 45kV and 30 mA, 173 mm goniometer circle, graphite monochromator, receiving slit width: 1 mm, divergence slit width: 1 mm, antiscatter slit width: 0.1 mm, soller slits 2.3 mm, stepscan,

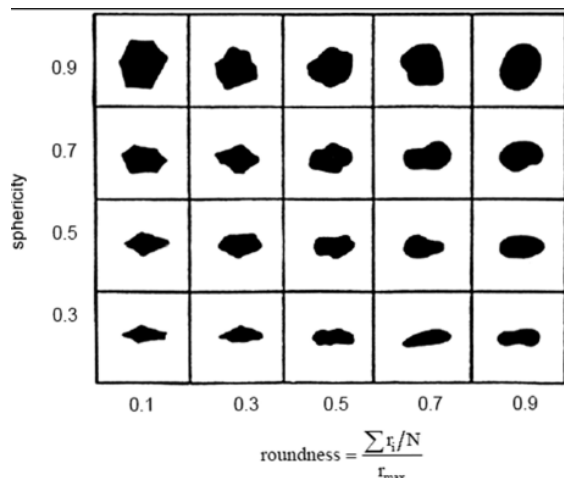
- Scan range: 5–65° (QUANTA users)
- Scan range: 3–75° (Rietveld users)
- Stepsize: 0.02
- Time/step: 2 seconds,
- Time/measurement: 1h50 min





4. Glauconite content and characterization

Glauconite content and characterization were measured and determined by means of visual inspection of thin sections. These thin sections were made by mixing a polyurethane powder with the sample and pressing them into pellets. Then, the surface of each pellet was polished to create crosscuts through the grains, and a thin section was made from a slice of the pellet. Images were taken with a standard optical microscope with transmitted light. All thin sections contained glauconite, quartz and K-feldspar. Opaque phases were present but only in very low proportions and were not identified. Sphericity and roundness of the grains were determined using the Krumbein/Sloss diagram given below.



LP1-01

Minerals	Volume (%)	Size (μm)	Sphericity	Roundness
Glauconite	35	100-250	0.7	0.7-0.9
Quartz	62	100-250	0.3	0.5
K-feldspar	2	100-250	0.7	0.5
Opaque	1	100-150	0.7	0.1
Other	<1	/	/	/

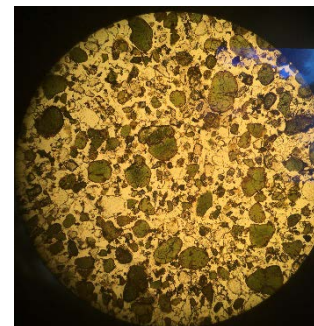
Remarks: low oxidation and weathering of glauconite



LP1-02

Minerals	Volume (%)	Size (μm)	Sphericity	Roundness
Glauconite	60	100-650	0.7-0.9	0.7-0.9
Quartz	37	100-650	0.5-0.7	0.3-0.5
K-feldspar	1	100-250	0.7	0.3-0.5
Opaque	1	100-250	0.7	0.3
Other	<1	/	/	/

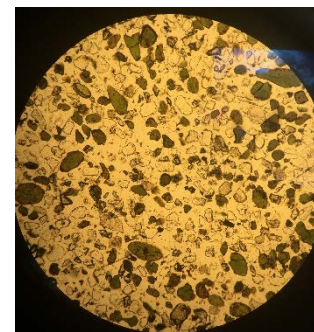
Remarks: moderate oxidation and weathering of glauconite



LP1-03

Minerals	Volume (%)	Size (μm)	Sphericity	Roundness
Glauconite	35	100-600	0.7	0.7
Quartz	62	100-600	0.7	0.3-0.5
K-feldspar	2	100-250	0.7	0.3-0.5
Opaque	1	100-250	0.7	0.1
Other	<1	/	/	/

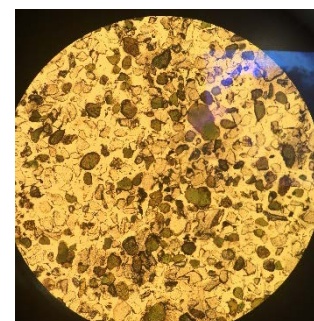
Remarks: low oxidation and weathering of glauconite



LP1-04

Minerals	Volume (%)	Size (μm)	Sphericity	Roundness
Glauconite	35	100-500	0.7-0.9	0.9
Quartz	63	100-500	0.7-0.9	0.3-0.5
K-feldspar	1	100-250	0.7-0.9	0.3-0.5
Opaque	1	100-250	0.7	0.1
Other	<1	/	/	/

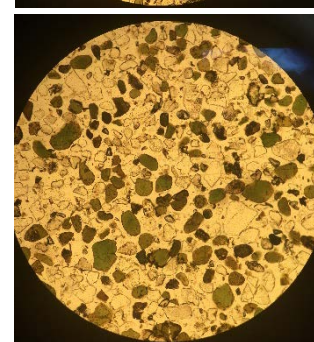
Remarks: low oxidation and weathering of glauconite



LP1-06

Minerals	Volume (%)	Size (μm)	Sphericity	Roundness
Glauconite	30	100-500	0.7-0.9	0.7-0.9
Quartz	68	100-500	0.7-0.9	0.5
K-feldspar	1	100-250	0.7-0.9	0.5
Opaque	1	100-250	0.7-0.9	0.3
Other	<1	/	/	/

Remarks: low oxidation and weathering of glauconite

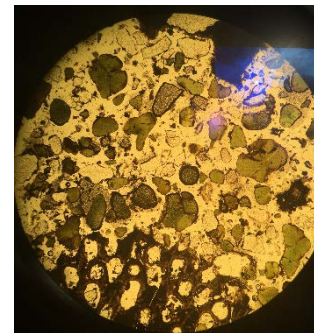


LP1-07

Minerals	Volume (%)	Size (μm)	Sphericity	Roundness
Glauconite	45	100-650	0.7-0.9	0.5-0.7
Quartz	33	100-500	0.7-0.9	0.3-0.5
K-feldspar	1	100-250	0.7-0.9	0.3-0.5
Opaque	1	100-250	0.7	0.1
Other	20	/	/	/

Remarks: Other also contains fossil fragments

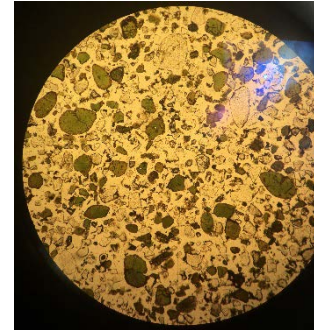
Strong oxidation and weathering of glauconite



LP1-08

Minerals	Volume (%)	Size (μm)	Sphericity	Roundness
Glauconite	45	100-650	0.5-0.7	0.7-0.9
Quartz	52	100-500	0.7-0.9	0.3
K-feldspar	1	100-250	0.7-0.9	0.3-0.5
Opaque	1	100-250	0.7	0.3
Other	<1	/	/	/

Remarks: Strong oxidation and weathering of glauconite



LP1-09

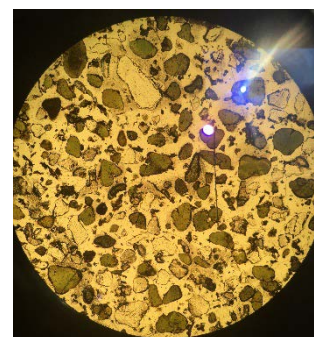
Minerals	Volume (%)	Size (μm)	Sphericity	Roundness
Glauconite	45	100-500	0.5-0.7	0.7-0.9
Quartz	63	100-500	0.7-0.9	0.3-0.5
K-feldspar	1	100-250	0.7-0.9	0.3-0.5
Opaque	1	100-250	0.7-0.9	0.1-0.3
Other	<1	/	/	/



Remarks: Moderate oxidation and weathering of glauconite

LP1-10

Minerals	Volume (%)	Size (μm)	Sphericity	Roundness
Glauconite	55	100-500	0.7-0.9	0.7-0.9
Quartz	43	100-500	0.7-0.9	0.3-0.5
K-feldspar	1	100-250	0.7-0.9	0.3-0.5
Opaque	1	100-250	0.7	0.3
Other	<1	/	/	/



Remarks: Moderate oxidation and weathering of glauconite

LP1-14

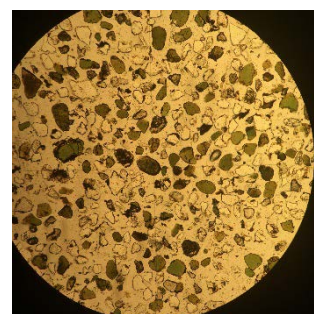
Minerals	Volume (%)	Size (μm)	Sphericity	Roundness
Glauconite	30	100-500	0.7-0.9	0.7-0.9
Quartz	68	100-500	0.7-0.9	0.3-0.5
K-feldspar	1	100-250	0.7-0.9	0.3-0.5
Opaque	1	100-250	0.9	0.1-0.3
Other	<1	/	/	/



Remarks: Low oxidation and weathering of glauconite

LP1-15

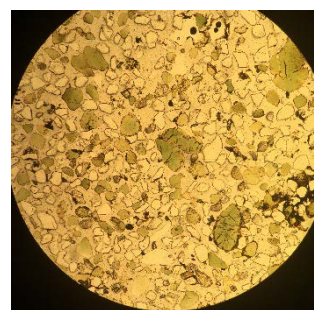
Minerals	Volume (%)	Size (μm)	Sphericity	Roundness
Glauconite	25	100-500	0.7-0.9	0.7-0.9
Quartz	63	100-500	0.7-0.9	0.3-0.5
K-feldspar	1	100-250	0.7-0.9	0.3-0.5
Opaque	1	100-250	0.7-0.9	0.1-0.3
Other	<1	/	/	/



Remarks: Moderate oxidation and weathering of glauconite

LP1-16

Minerals	Volume (%)	Size (μm)	Sphericity	Roundness
Glauconite	30	100-500	0.7-0.9	0.7-0.9
Quartz	68	100-500	0.7-0.9	0.3-0.5
K-feldspar	1	100-250	0.7-0.9	0.3-0.5
Opaque	1	100-250	0.7	0.1
Other	<1	/	/	/



Remarks: Low oxidation and weathering of glauconite

LP1-18

Minerals	Volume (%)	Size (μm)	Sphericity	Roundness
Glauconite	40	100-500	0.7-0.9	0.7-0.9
Quartz	58	100-500	0.7-0.9	0.3-0.5
K-feldspar	1	100-250	0.7-0.9	0.3-0.5
Opaque	1	100-250	0.7-0.9	0.1-0.3
Other	<1	/	/	/

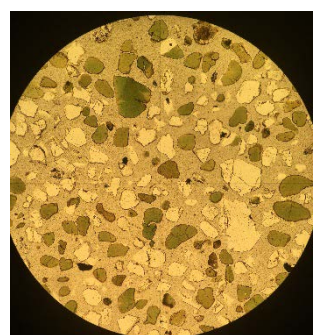
Remarks: Low oxidation and weathering of glauconite



LP1-19

Minerals	Volume (%)	Size (μm)	Sphericity	Roundness
Glauconite	40	100-500	0.7-0.9	0.7-0.9
Quartz	57	100-500	0.7-0.9	0.3-0.5
K-feldspar	2	100-250	0.7-0.9	0.3-0.5
Opaque	1	100-250	0.7-0.9	0.1-0.3
Other	<1	/	/	/

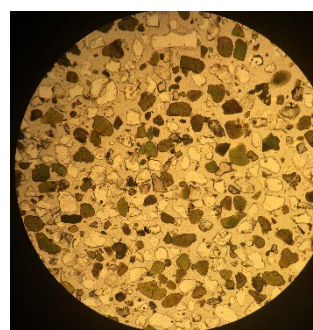
Remarks: moderate to strong oxidation and weathering of glauconite



LP1-20

Minerals	Volume (%)	Size (μm)	Sphericity	Roundness
Glauconite	49	100-400	0.7-0.9	0.7-0.9
Quartz	49	100-400	0.7-0.9	0.3-0.5
K-feldspar	1	100-250	0.7-0.9	0.3-0.5
Opaque	1	100-250	0.7-0.9	0.1-0.3
Other	<1	/	/	/

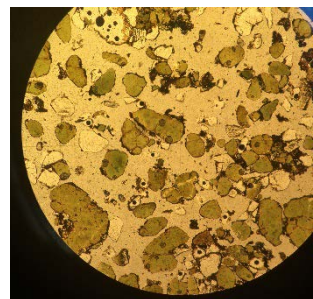
Remarks: Very strong oxidation and weathering of glauconite



LP1-26

Minerals	Volume (%)	Size (μm)	Sphericity	Roundness
Glauconite	60	100-700	0.7-0.9	0.7-0.9
Quartz	36	100-700	0.7-0.9	0.3-0.5
K-feldspar	3	100-250	0.7-0.9	0.3-0.5
Opaque	1	100-250	0.7-0.9	0.1-0.3
Other	<1	/	/	/

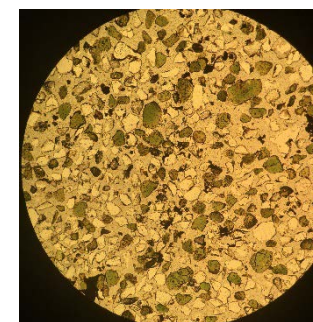
Remarks: Strong oxidation and moderate weathering of glauconite



LP2-15

Minerals	Volume (%)	Size (μm)	Sphericity	Roundness
Glauconite	30	100-500	0.7-0.9	0.7-0.9
Quartz	67	100-500	0.7-0.9	0.3-0.5
K-feldspar	1	100-250	0.7-0.9	0.3-0.5
Opaque	2	100-250	0.7-0.9	0.1-0.3
Other	<1	/	/	/

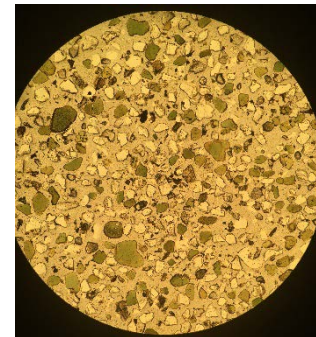
Remarks: Moderate oxidation and weathering of glauconite



LP2-16

Minerals	Volume (%)	Size (μm)	Sphericity	Roundness
Glauconite	30	100-500	0.7-0.9	0.7-0.9
Quartz	67	100-500	0.7-0.9	0.3-0.5
K-feldspar	2	100-250	0.7-0.9	0.3-0.5
Opaque	1	100-250	0.7-0.9	0.1-0.3
Other	<1	/	/	/

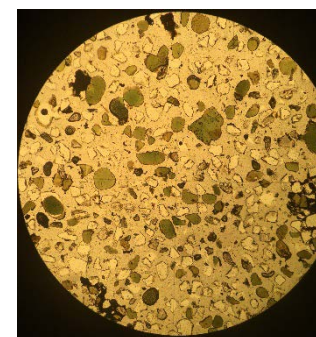
Remarks: Low oxidation and weathering of glauconite



LP2-17

Minerals	Volume (%)	Size (μm)	Sphericity	Roundness
Glauconite	30	100-500	0.7-0.9	0.7-0.9
Quartz	68	100-500	0.7-0.9	0.3-0.5
K-feldspar	1	100-250	0.7-0.9	0.3-0.5
Opaque	1	100-250	0.7-0.9	0.1-0.3
Other	<1	/	/	/

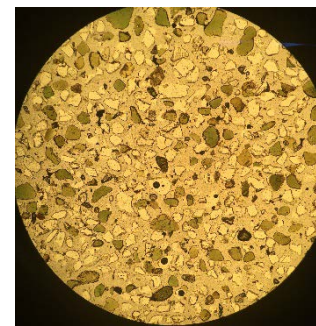
Remarks: Low oxidation and weathering of glauconite



LP2-18

Minerals	Volume (%)	Size (μm)	Sphericity	Roundness
Glauconite	30	100-500	0.7-0.9	0.7-0.9
Quartz	66	100-500	0.7-0.9	0.3-0.5
K-feldspar	3	100-250	0.7-0.9	0.3-0.5
Opaque	1	100-250	0.7-0.9	0.1-0.3
Other	<1	/	/	/

Remarks: Low oxidation and weathering of glauconite



LP2-19

Minerals	Volume (%)	Size (μm)	Sphericity	Roundness
Glauconite	30	100-500	0.7-0.9	0.7-0.9
Quartz	68	100-500	0.7-0.9	0.3-0.5
K-feldspar	1	100-250	0.7-0.9	0.3-0.5
Opaque	1	100-250	0.7-0.9	0.1-0.3
Other	<1	/	/	/

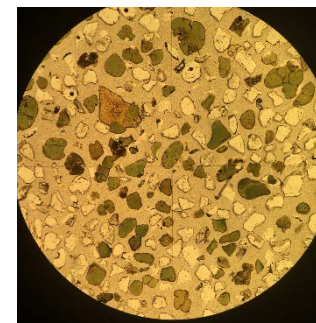
Remarks: Low oxidation and weathering of glauconite

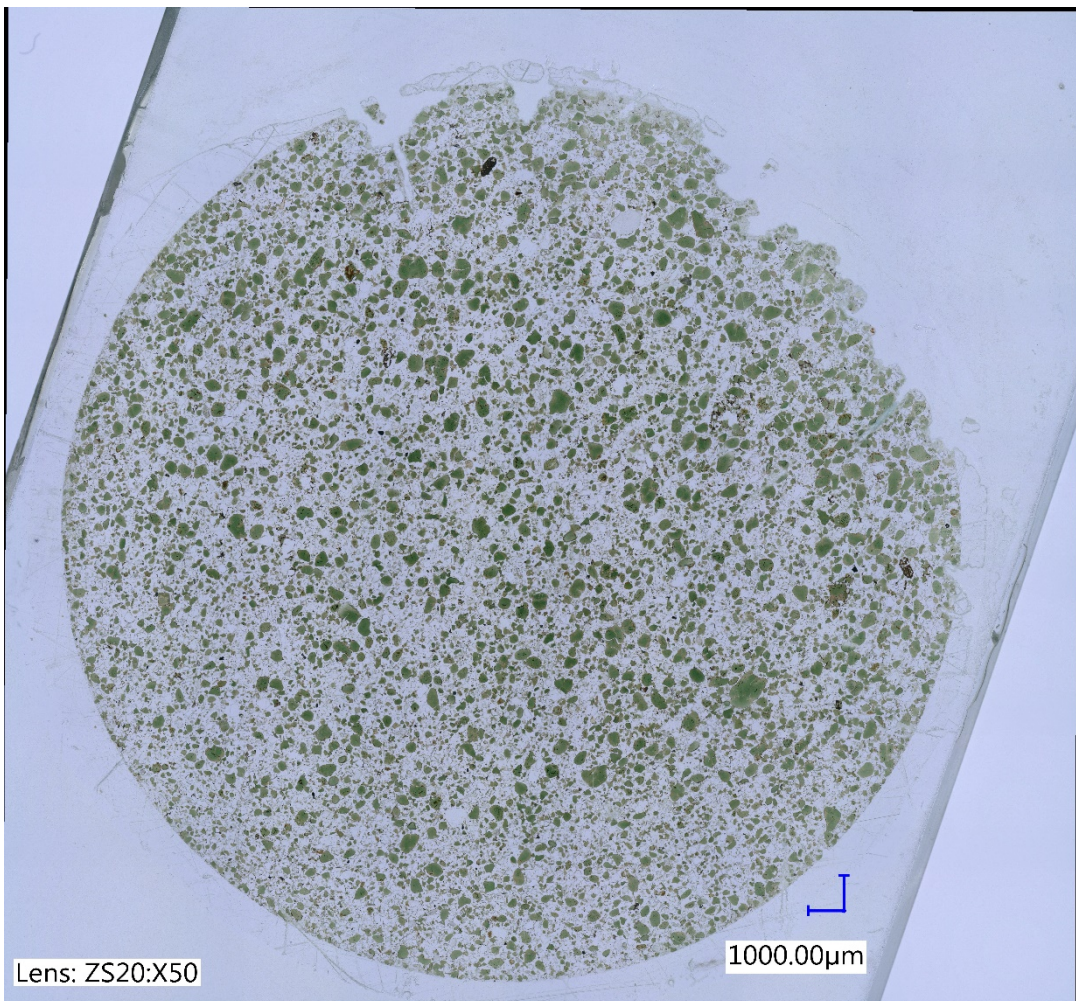


LP2-50

Minerals	Volume (%)	Size (μm)	Sphericity	Roundness
Glauconite	30	100-500	0.7-0.9	0.7-0.9
Quartz	68	100-500	0.7-0.9	0.3-0.5
K-feldspar	1	100-250	0.7-0.9	0.3-0.5
Opaque	1	100-250	0.7-0.9	0.1-0.3
Other	<1	/	/	/

Remarks: Low oxidation and weathering of glauconite





High resolution image of thin-section DE18VH02 (Sample LP1-02)

4. Granulometry: statistical analysis of grain size

Overview of statistical values of grainsize analysis. Many samples had a bimodal distribution with a finer (1) and a coarser peak (2). Sorting was calculated based on Folk & Ward (1957). S.D.: standard deviation.

Sample N°	Depth in section	Mean 1	Mean 2	S.D. 1	S.D. 2	Mode 1	Mode 2	Sorting according to Folk & Ward 1	Sorting according to Folk & Ward 2
	M	µm	µm	µm	µm	µm	µm	Φ	ϕ
LP1-50	2.7	200	/	1.7	/	224	/	0.8	/
LP1-61	3.8	92	461	3.6	1.1	169	472	1.8	0.14
LP1-62	4.2	112	459	2.9	1.1	169	472	1.5	0.14
LP1-63	4.8	66	468	3.7	1.2	154	472	1.9	0.26
LP1-64	5.0	125	/	2.5	/	169	/	1.3	/
LP1-26	1.5	39	/	7.6	/	224	/	2.9	/
LP2-15	4.0	109	433	2.7	1.1	169	472	1.4	0.19
LP2-16	4.2	121	443	2.7	1.1	169	472	2.7	0.18
LP2-17	4.4	118	460	2.9	1.1	169	472	1.5	0.14
LP2-18	4.7	143	454	2.3	1.1	169	472	1.2	0.14
LP2-19	5.2	155	/	2.0	/	169	/	1.0	/
LP1-01	0.3	92	/	3.7	/	169	/	1.9	/
LP1-02	0.4	136	/	3.2	/	186	/	1.7	/
LP1-03	0.6	125	457	2.4	1.1	154	472	1.3	0.16
LP1-04	0.9	137	465	2.3	1.1	169	472	1.2	0.13
LP1-06	1.3	193	/	1.9	/	204	/	1.0	/
LP1-07	1.5	131	/	4.5	/	270	/	2.2	/
LP1-08	1.6	128	/	3.2	/	169	/	1.7	/
LP1-09	1.7	104	/	3.5	/	169	/	1.8	/
LP1-10	1.9	86	/	5.8	/	270	/	2.5	/
LP1-11	2.5	121	/	2.9	/	154	/	1.5	/
LP1-12	3.0	183	/	2.7	/	224	/	1.4	/
LP1-13	3.5	93	/	3.6	/	169	/	1.9	/
LP1-14	3.7	117	458	2.9	1.1	154	472	2.9	0.14
LP1-15	4.2	128	455	2.6	1.1	169	472	1.4	0.16
LP1-16	4.5	111	/	2.9	/	169	/	1.5	/
LP1-17	5.0	175	/	2.1	/	186	/	1.1	/
LP1-18	5.2	243	/	1.6	/	246	/	0.7	/
LP1-19	5.5	235	/	1.7	/	246	/	0.8	/
LP1-20	6.1	211	/	2.0	/	246	/	1.0	/

5. Additional references

Folk, R.L. & Ward, W.C., 1957. Brazos River Bar: a study in the significance of grain size parameters. *Journal of Sedimentary Petrology*, 27/1, 3–26. <https://doi.org/10.1306/74D70646-2B21-11D7-8648000102C1865D>

Fritz, S.F. & Popp, R.K., 1985. A single-dissolution technique for determining FeO and Fe₂O₃ in rock and mineral samples. *American Mineralogist* 70/9-10, 961–968.

Shapiro, L., 1960. A spectrophotometric method for the determination of FeO in rocks. U.S. Geological Survey Professional Paper, 400B, 496–497.